Macromolecules

ARTICLE

pubs.acs.org/Macromolecules

Thermodynamics of Photoresponsive Polyelectrolyte−Dye Assemblies with Irradiation Wavelength Triggered Particle Size

Immanuel Willerich and Franziska Gröhn*

Department of Chemistry and Pharmacy and Interdisciplinary Center for Molecular Materials, Friedrich-Alexander-University Erlangen-Nürnberg, Egerlandstrasse 3, 91058 Erlangen, Germany

ABSTRACT: Electrostatic self-assembly of polyelectrolytes and photoresponsive dye counterions can yield supramolecular nanoparticles in aqueous solution, the size of which can be controlled through light irradiation with varying wavelengths. Nanoparticles are formed from fourth-generation poly(amido amine) dendrimers and an excess of the oppositely charged anionic diazo dyes Acid Yellow 38 (Ay38) or Direct Yellow 12 (Dy12). Particle stability is provided by a negative particle charge originating from excess anionic dye. Irradiation with UV light leads to partial isomerization of the trans-dye to the cis-isomer. The degree of isomerization controls the size continuously and very precisely, enabling particle radii between 30 and 250 nm. Quantitative insight is based on surface area, charge density, and thermodynamics of the dye binding. Dynamic light scattering (DLS) and zeta-potential measurements have been used to study size and stabilization, and isothermal titration calorimetry (ITC) was applied to determine enthalpies, stoichiometry parameters, and equilibrium constants of trans- and cis-dye binding to the macroion.

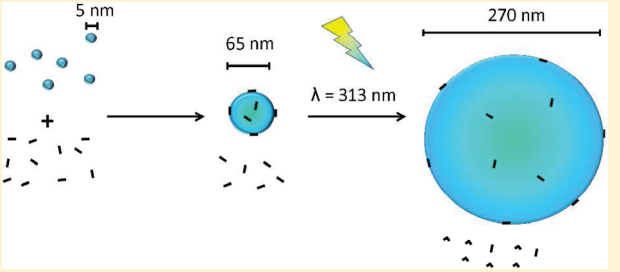

INTRODUCTION

Functional supramolecular nanoparticles are a rapidly growing field due to the wide range of applications, whereby polymers are often important building blocks.[1−13] Recent emerging applications of nanoparticles in composite materials,[14−16] carrier systems,[17,18] or optoelectronics[19,20] often require the ability to respond to external triggers. Supramolecular chemistry in polymer science has opened up many viable roads toward responsive nanoparticles for such applications due to great variety of usable interaction forces like for example $\pi-\pi$ stacking,[21−25] amphiphilicity,[26−29] or ionic interactions.[30−33] These are in most cases weaker than covalent bonds and thus often susceptible to relatively soft external triggers. The variety of supramolecular interactions can lead to various types of nanostructures, which is promising in view of the applications mentioned above. Especially amphiphilic molecules can lead to micelles, vesicles, or bilayers and many other structural motifs.[26−29] However, there is still a need for new concepts that can fulfill three basic criteria at once: precise size control of the final structure, responsiveness to soft triggers like light or temperature, and avoidance of very specific binding patterns that have to be created with high synthetic effort. Consequently, the development of new supramolecular routes toward nanoparticles fulfilling these criteria is promising to create new types of functional structures.

There are several possible triggers like temperature, pH, or light to influence size, structure, and properties of nanostructures. Especially light-triggered systems have received a lot of attention due to the noninvasiveness of this trigger, which lead to a variety of elegant structures.[34−46] For example, self-assembled functionalized small nanoparticles can be photo-cross-linked into larger colloidal particles by dimerization of a cinnamic acid derivative.[39,40] Other systems are based on photoresponsive surfactants, which can for example undergo isomerization, photodestruction, or dimerization in UV light, inducing morphological changes in solution.[41,45,46] Photoresponsivity based on cis−trans-isomerization of azobenzene moieties on irradiation with UV light is a versatile route toward responsive nanostructures. In a system consisting of sodium dodecyl sulfate and a surfactant bearing an azo moiety, vesicle to micelle or vesicle to lamellae transitions were observed.[42,43] Recently, transitions between vesicles, spherical micelles, and rodlike micelles formed by a surfactant/dye mixture were described.[44] These morphology changes are attributed to the change in the polarity of the compounds. Other examples are photoswitchable supramolecular dye−hydrogel composites that are able to respond to light with contraction or expansion due to a change in hydrophobicity of the dye[47] or azobenzene-bearing polyetheramine particles that can change their size and shape due to differences in packing between the cis- and trans-isomer.[48] In addition, the difference in complexation behavior between *trans*- and *cis*-azobenzene by cyclodextrin can be exploited to generate light-responsive supramolecular particles.[49,50]

In this study, we report an approach toward photoresponsive nanoparticles based on electrostatic self-assembly of polyelectrolytes and organic counterions, which is a concept to produce nanoparticles in the size range of 100 nm incorporating multiple polyelectrolyte molecules per particle.[51−62] In the case of organic dye molecules as counterions, electrostatic interactions between the oppositely charged organic dye counterion and the

Received: March 10, 2011
Revised: April 15, 2011
Published: May 03, 2011

Scheme 1. (top) Building Blocks for Electrostatic Self-Assembly Used in This Study; (bottom) Simplified Sketch of the Assembly Formation from the Individual Building Blocks[a]

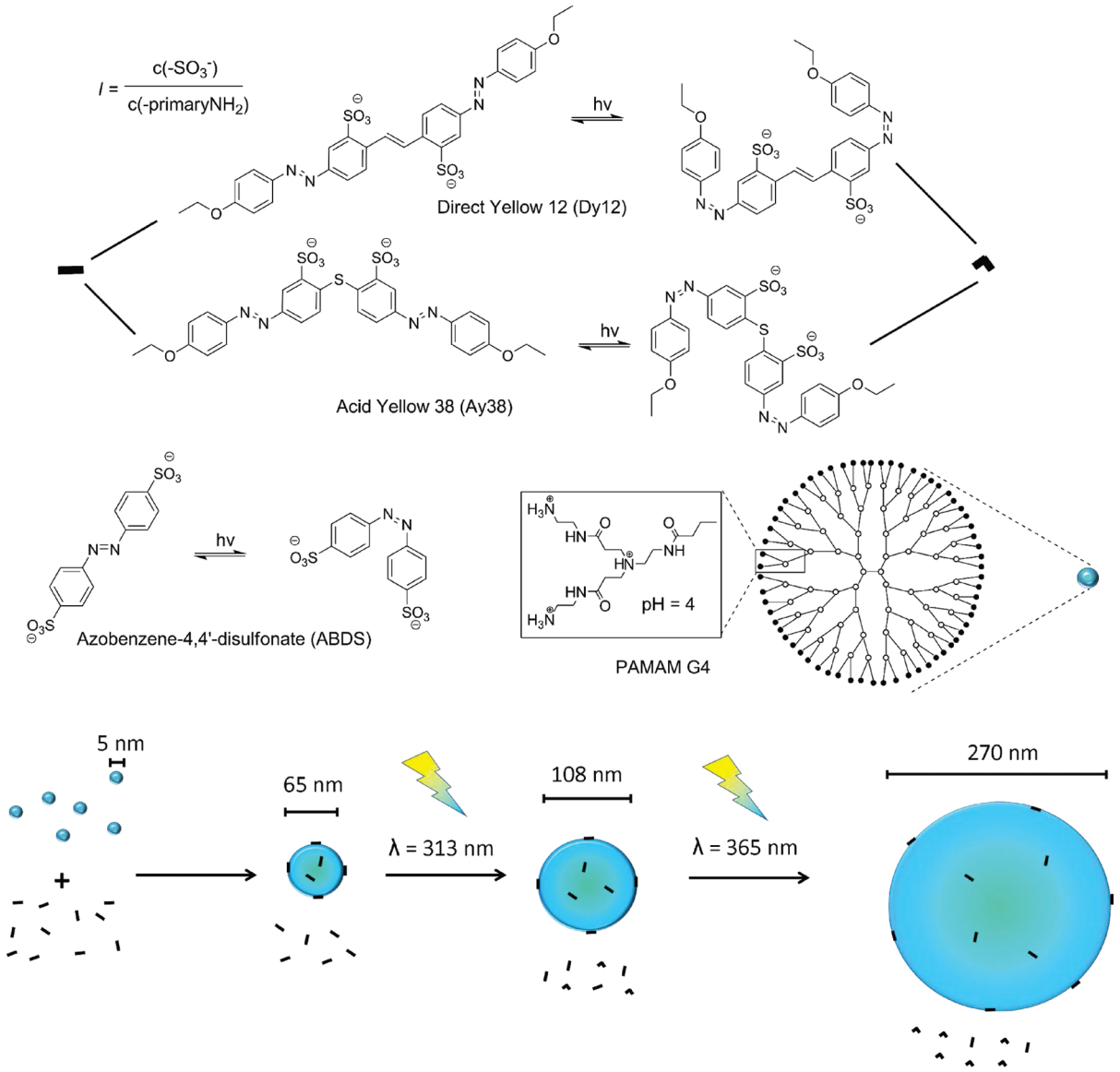

[a] Black short lines represent simplified trans-, V-shaped objects simplified cis-dye molecules. Dye molecules are smaller than indicated by the scale and enlarged for clarity.

macroion lead to electrostatic binding of the dye molecules to the polyelectrolyte. Additionally, mutual $\pi-\pi$-stacking in-between the dye counterions occurs. This leads to the interconnection of individual polymer molecules into larger assemblies with more than 10-fold size as compared to individual polymer molecules. Photoresponsiveness of the structures is enabled by using photoisomerizeable azo dyes. In a recent communication, we phenomenologically investigated electrostatically self-assembled nanoparticles consisting of an anionic azo dye and cationic polyamidoamine dendrimers.[60] The building blocks Acid Yellow 38 (Ay38) and generation four poly(amido amine) (PAMAM) dendrimer are depicted in Scheme 1. The outcome of that study was that electrostatically self-assembled nanoparticles consisting of cationic dendrimer and an excess of anionic Ay38 dye in the trans form (without irradiation no cis-dye is present) could change their size on exposure to UV light from a dendrimer−dye ratio dependent starting size of 50−100 nm to sizes up to 500 nm. A negative particle charge turned out to be decisive for the stability of the initial small particles and responsible for irradiation-induced size changes. Particles are negatively charged as there is an excess of anionic trans-dye molecules, which is partially free in solution and partially bound overstoichiometrically to the dendrimer−dye assemblies. Overstoichiometrically means that further dye molecules bind to the assembly even though all primary and tertiary amino groups are already ion-paired with dye sulfonate groups. The particles are electrostatically stabilized. Irradiation leads to conversion of the trans-dye to the cis-state. Previously, we postulated that cis-dye may have a lower ability to bind overstoichiometrically and thus to stabilize the particles. Consequently, the lower negative net charge of the particles leads to a size increase. The difference in overbinding

dx.doi.org/10.1021/ma200538e |*Macromolecules* 2011, 44, 4452–4461

ability of trans- and cis-dye hence is a crucial effect, which is elucidated by thermodynamic investigations in this study.

After the previous mostly phenomenologic report, the objective of this study is to assess the driving forces quantitatively to further understand the role of charge and trans−cis isomerization in the light-driven size-control process. In this context, more detailed insights can be acquired by investigating particles formed with different azo dyes. This also allows to further establish the concept as a new versatile route toward light-triggered size-controllable nanoparticles in solution.

EXPERIMENTAL SECTION

Chemicals. Generation 4 poly(amido amine) dendrimer was obtained from Dendritech, Midland, MI.[63] Radius and size distribution given by the supplier were confirmed by DLS and HPLC. Acid Yellow 38 in 40% grade and Direct Yellow 12 as rare chemical were obtained from Sigma-Aldrich, Schnelldorf, Germany. Acid Yellow 38 was recrystallized five times from an aqueous solution of sodium acetate (35 w%) followed by five recrystallization steps from ethanol, yielding a salt-free product with >98 wt % content.[64] Purity of both dyes was checked by elemental analysis and extinction coefficient. No detectable organic impurities remain by this procedure. Azobenzen-4,4′-disulfonate was synthesized from sulfanilic acid and hypochlorite following a procedure by Clarke and purified likewise Ay38.[65]

Sample Preparation. Stock solutions were prepared in Milli-Q ultrapure water (>18.2 MΩ/cm). A solution of the dye at pH = 10.5 was diluted with Milli-Q ultrapure water adjusted to pH = 10.5. Dendrimer stock solution at the same pH was added. After mixing, the appropriate amount of HCl was added at once under turbulent mixing to adjust the sample pH to 3.5 inducing assembly formation. pH values were adjusted by adding the calculated amount of NaOH or HCl standard solutions. All pH values were counter-checked by a freshly calibrated pH electrode. The standard dendrimer concentration in this study was $c = 0.009\ \mathrm{g\ L^{-1}}$.

Light Scattering. Measurements were carried out using an ALV 5000 correlator with 320 channels (ALV GmbH, Langen, Germany) and a HeNe laser with a wavelength of $\lambda = 632.8$ nm with 22 mW output power. A range of scattering angles of $30° \leq \theta \leq 150°$ was covered. Measurement and data analysis were as established: The time autocorrelation function of the scattered intensity was measured and converted into the electric field autocorrelation function via Siegert relation. The electric field autocorrelation functions were analyzed by inverse Laplace transformation using the program CONTIN by Provencher[66] or by stretched exponential fits. The apparent diffusion coefficient was calculated from the inverse relaxation time and extrapolated to zero scattering vector square. Hydrodynamic radii were obtained via Stokes−Einstein relation from diffusion coefficients.

ζ-Potential. ζ-potential measurements were conducted on a on a DelsaNano C Particle Analyzer (Beckmann Coultier, Krefeld, Germany). Usually three runs were used. The Smoluchowski formula was used to calculate electrophoretic mobility and ζ-potential as there is about 1 mmol low molecular mass salt in the solution from pH adjustment.

UV−vis Spectroscopy. Absorption spectra were recorded on a Cary 5000 spectrometer from Varian using quartz cuvettes with 1 cm path length.

Isothermal Titration Calorimetry. Isothermal titration calorimetry was performed on a VP-ITC microcalorimeter from MicroCal, Northampton, MA. As control, dilution experiments of the individual components (Ay38, Dy12, ADBS, G4 PAMAM) were carried out. For the dye-dilution experiment, one initial injection of 10 μL to saturate the titration cell wall (as azo dyes tend to adsorb to the inner surface of the Hastelloy cell) was followed by 20 injections of 5 μL each. Dilution heats were found not to play a role in the system under investigation facilitating the analysis. For dendrimer−dye experiments, 20−25 injections of 10−15 μL each were used. The time span between subsequent injections was 300 s. All experiments were conducted at 25 °C. Formic acid/formiate was used as buffer system with c(buffer) = 15 mmol. Data analysis was performed with the modified model described below implemented in the MicroCal ITC data analysis software for Origin 7.0

Sample Irradiation. Samples prepared according to the procedure described above were irradiated on a Horiba Yvon Jobin Fluoromax spectrometer. The bandpass filter was set to $x \pm 20$ nm whereby x is the irradiation wavelength. Irradiation was carried out for 20 min. It was checked that longer irradiation times did not influence the results; i.e., the photostationary state was reached.

AFM. For AFM, solutions were drop-cast on 3-aminopropyltriethoxysilane (APTES)-modified mica and blow-dried. Modification was carried out by deposition of 15 μL of an 0.05 wt % APTES solution on freshly cleaved mica. After 15 min, the surface was rinsed and blow-dried followed by depositon of 15 μL sample solution. The deposition time was 1 min. After that, the surface was rinsed with 5 mL of water of the same pH as the sample and blow-drying concluded the sample preparation procedure. AFM images were recorded on a NanoSurf Easy Scan instrument (Boston, MA) in tapping mode.

RESULTS AND DISCUSSION

Dendrimer−dye samples are characterized by their loading ratio, i.e., the molar ratio of dye sulfonate groups to primary dendrimer amino groups (eq I). As the titration curve of PAMAM dendrimer is known, this chemically defined ratio can be translated in the charge ratio easily.[54] For pH = 3.5, charge stoichiometry is located at a loading ratio of $l = 2$.

$$l = \frac{c(-\mathrm{SO_3^-})}{c(-\mathrm{primary\ NH_2})} \qquad \text{(I)}$$

To study the response of dye−dendrimer nanoparticles to UV light, samples with excess of Acid Yellow 38 (Ay38) or Direct Yellow 12 (Dy12) are prepared ($l \approx 4$, compare eq I) and subsequently irradiated with light of different wavelengths. Changes in size, charge, and thermodynamic parameters are investigated. In section A, we investigate the photophysical behavior of the azo dyes depicted in Scheme 1, i.e., the photoinduced trans−cis and the thermal cis−trans isomerization equilibria at different irradiation wavelengths using absorption spectroscopy. Especially the amount of trans- and cis-isomers of the dyes are investigated at different irradiation wavelengths as those are key to understanding the size changes of the assemblies. Section B comprises investigations of size and structure evolution of nanoparticles from Ay38 or Dy12 and dendrimer by atomic force microscopy (AFM) and dynamic light scattering (DLS) depending on the irradiation wavelength. In addition, changes in particle charge are monitored by ζ-potential measurements. Section C serves to investigate driving forces for the size-control process by isothermal titration calorimetry (ITC) to further understand the findings from section B.

A. Photophysical Characterization of the Azo-Dye Building Blocks by Absorption Spectroscopy. To investigate nanoparticle size changes on irradiation, knowledge about the isomerization process is key as the different behavior of trans- and cis-isomer turned out to be the cause for the nanoparticle size changes.[60] Using a method by Fischer, in which a dye solution is irradiated at two different wavelengths and the absorption spectra are measured, we estimated the fraction of photoisomerized dye, $\chi_{\mathrm{cis}}(\lambda_{\mathrm{irr}})$, at a particular irradiation wavelength. Using eq II, we determined the absorption spectrum of the pure cis-dye

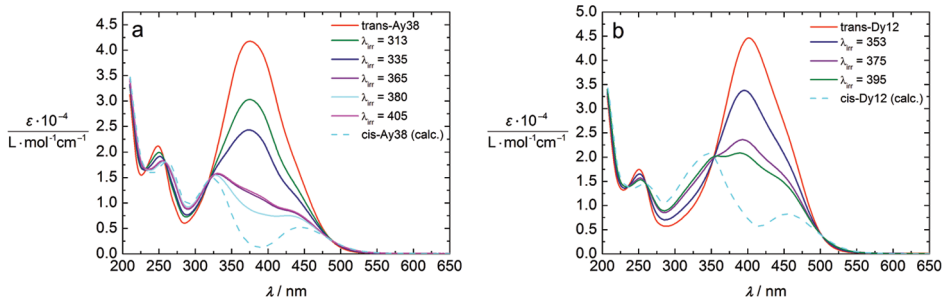

Figure 1. Absorption spectra of (a) Ay38 (c = 0.0127 mmol/L) and (b) Dy12 (c = 0.0211 mmol/L) after irradiation with light of different wavelengths.

Table 1. Dye Isomerization Data for BS, Ay38, and Dy12

dye	λ_{irr}/nm	$\chi_{cis}(\lambda)$	$\chi_{cisITC}(\lambda)^a$
Ay38	–	0	0
Ay38	313	0.29	
Ay38	335	0.44	
Ay38	365	0.75	
Ay38	380	0.83	0.66
Dy12		0	0
Dy12	353	0.30	0.36
Dy12	375	0.57	
Dy12	395	0.65	0.45

[a] Compare section C.

of Ay38 and Dy12.[67,68]

$$\varepsilon_{cis}(\lambda) = \varepsilon(\lambda) - (1 - \chi_{cis}(\lambda_{irr}))\varepsilon_{trans}(\lambda) \qquad (II)$$

λ and λ_{irr} are the wavelength for which the extinction coefficient is determined and the irradiation wavelength, respectively; $\varepsilon_{cis}(\lambda)$ and $\varepsilon_{trans}(\lambda)$ are the extinction coefficients of the pure cis- and trans-isomer at a particular wavelength, whereas $\varepsilon(\lambda)$ is the extinction coefficient of the mixture of isomers in photoequilibrium at a certain irradiation wavelength.

Figure 1 depicts absorption spectra of Ay38 (a) and Dy12 (b) before and after irradiation with light at a set of different wavelengths between λ_{irr} = 300 and λ_{irr} = 405 nm. The calculated spectra of cis-Ay38 and cis-Dy12 are represented by the dashed lines. Knowing the cis-spectra, the degree of isomerization ($x_{cis}(\lambda_{irr})$) of the dyes in this mixture of two species at any irradiation wavelength between λ_{irr} = 313 and λ_{irr} = 420 nm can be determined from the particular absorption spectrum of the dye solution according to eq II. These data are depicted in Table 1. In general, the highest degrees of isomerization of 0.83 for Ay38 and 0.65 for Dy12 can be achieved by irradiating close to the absorption maximum of the trans-isomer (λ_{irr} = 380 nm for Ay38 and λ_{irr} = 395 nm for Dy12). That is, as the cis-isomer has a minimum in absorbance close to the maximum of the trans-isomer due to the band splitting of the former. For Dy12, the extinction coefficient for the cis-isomer is higher than for Ay38, which is the reason for the lower maximum degree of isomerization as the maximum degree of isomerization is proportional to the ratio of the extinction coefficients of the trans- and cis-form of the dyes for both isomers. Irradiation at the isosbestic points of Ay38/Dy12 leads to a fraction of cis-dye lower than half, which shows that the quantum yield for the trans−cis isomerization is lower than for the reverse process.

Irradiation with light at wavelengths below λ_{irr} = 300 nm was avoided, as undesirable decomposition may occur on irradiation with light of lower wavelengths. Thermal cis−trans isomerization can be neglected in photoequilibrium as this process is much slower than the photoinduced process.

Futhermore, the knowledge of the thermal reisomerization constant $k_{cis\text{-}trans}$ is crucial to know to estimate whether the cis-form is stable enough to be appropriate for the present application. It can be determined by fitting the reisomerization kinetics with an exponential decay function as depicted in eq III:

$$c(\text{cis-dye}) = c_0(\text{cis-dye})\ \exp(-k_{cis\text{-}trans}t) \qquad (III)$$

$k_{cistrans}$(Ay38) was already determined to $k_{cistrans}$(Ay38) = 1.63×10^{-5} 1/s ($t_{1/2}$ = 11.84 h) previously.[60,68] For Dy12, we calculated a thermal cis−trans reisomerization constant of $k_{cistrans}$ (Dy12) = 3.86×10^{-5} 1/s ($t_{1/2}$ = 4.99 h). The relaxation time for Dy12 is much smaller than for Ay38, likely due to the conjugation of the π-system provided by the ethylene group as compared to the isolated π-systems in Ay38 due to the linkage of both azobenzene moieties by the sulfur atom. Still, 5 h is appropriate for the experiments herein as the size change kinetics is much faster. In conclusion, especially for Ay38, the fraction of isomerized dye can be varied in small steps depending on the wavelength used for irradiation.

B. Dependency of Particle Size and Charge on the Degree of Isomerization. Light scattering and atomic force microscopy can yield information about size and shape of the assemblies, which is the basis for a thorough analysis of the dendrimer−dye nanoparticles, especially to clarify the way the light-induced growth process is controlled.

As elucidated in Table 1, the degree of isomerization varies between χ_{cis} = 0.29 and χ_{cis} = 0.83 for Ay38 and between χ_{cis} = 0.30 and χ_{cis} = 0.65 for Dy12 depending on the irradiation wavelength for pure dye samples. To study the influence of the trans−cis isomerization on particle size and charge, samples with moderate excess of Ay38 (l = 3.59) and Dy12 (l = 4.19) were prepared and irradiated sequentially with ascending wavelength and characterized by dynamic light scattering and ζ-potential measurements. Results are shown in Table 2. For Ay38, AFM was performed with a sample with l = 4.03, and the same irradiation routine followed described above. We chose an excess of dye (l > 2) as the previous phenomenological study showed that samples with excess of dendrimer do not exhibit a photoresponsive particle size upon UV-irradiation apart from a narrowing size distribution. Hence, excess dye molecules are crucial for the size-change mechanism.[60]

It is assumed that the presence of dendrimer−dye assemblies does not influence the photophysical behavior of the free excess

Table 2. Structural Data for ABDS, Ay38, and Dy12/G4 Dendrimer Assemblies

dye	λ_{irr}/nm	c_{total}/(mol/L)	c_{excess}[a]/(mol/L)	$c_{free\text{-}cis}$[a]/(mol/L)	$c_{free\text{-}trans}$[a]/(mol/L)	R_h DLS/nm
Ay38	–	7.74×10^{-5}	3.49×10^{-5}	0	3.49×10^{-5}	33
Ay38	313	7.74×10^{-5}	3.49×10^{-5}	1.00×10^{-5}	2.49×10^{-5}	54
Ay38	335	7.74×10^{-5}	3.49×10^{-5}	1.54×10^{-5}	1.95×10^{-5}	74
Ay38	365	7.74×10^{-5}	3.49×10^{-5}	2.62×10^{-5}	8.70×10^{-6}	137
Ay38	380	7.74×10^{-5}	3.49×10^{-5}	2.90×10^{-5}	5.93×10^{-6}	251
Dy12		8.29×10^{-5}	4.37×10^{-5}	0	4.37×10^{-5}	34
Dy12	353	8.29×10^{-5}	4.37×10^{-5}	1.31×10^{-5}	3.06×10^{-5}	34
Dy12	375	8.29×10^{-5}	4.37×10^{-5}	2.49×10^{-5}	1.86×10^{-5}	64
Dy12	395	8.29×10^{-5}	4.37×10^{-5}	2.83×10^{-5}	1.52×10^{-5}	142

[a] Data for the samples from section B.

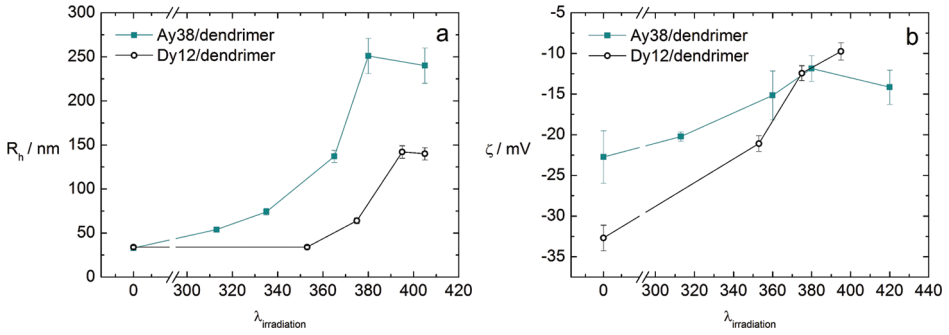

Figure 2. (a) Dependence of size (hydrodynamic radius R_h) and (b) charge (ζ-potential) on irradiation wavelength (degree of isomerization): l(Ay38) = 3.59, c(Ay38) = 7.75×10^{-5} mol/L; l(Dy12) = 4.19, c(Dy12) = 8.77×10^{-5} mol/L.

dye that is not incorporated in the particles, i.e., that the excess dye in solution is isomerized to the same extent as without the presence of polymer as the environment of the unbound amount of the dye (column c_{excess}, Table 2) is not different with regard to pure dye samples. Before, different samples of Ay38/dendrimer with different loading ratios were prepared and irradiated at 380 nm leading to the same degree of isomerization for samples with different loading ratios.[60] The new procedure allows to gradually increase the degree of isomerization.

Dynamic light scattering results for both Ay38 and Dy12 are displayed in Figure 2a. It shows that the hydrodynamic radius increases from R_h = 33 nm to R_h = 251 nm for Ay38 and R_h = 34 nm to R_h = 142 nm for Dy12, while the fraction of cis-dye in solution increases from 29% to 83% for Ay38 and from 30% to 65% for Dy12. This demonstrates that the concept to trigger the size of electrostatically self-assembled dendrimer−dye nanoparticles by means of UV light is not a special case for Ay38 but generally applicable for other photoisomerizable azo-dyes. The comparison of Ay38 and Dy12 shows that the size is directly connected to the degree of isomerization and in turn to the absolute concentration of the cis- and trans-isomers, provided that the absolute concentration and the loading ratio of the samples is comparable. That is, the concentration of residual trans-dye in solution determines the extent of the size change very precisely, allowing for a stepwise size increase. For Dy12, the maximum degree of isomerization is lower than for Ay38 and consequently the maximum size observed is smaller than for Ay38 (R_h = 142 nm vs R_h = 251 nm).

Varying the absolute concentration of the dendrimer and thereby, as the loading ratio is kept constant the concentration of dye, reveals further insight into the irradiation controlled size change process. For dendrimer concentrations of about half of the concentration applied above (c = 0.004 g L^{-1}), the initial assembly sizes and relative size changes were very similar to the values reported. A 10% concentration (0.001 g L^{-1}), in contrast,

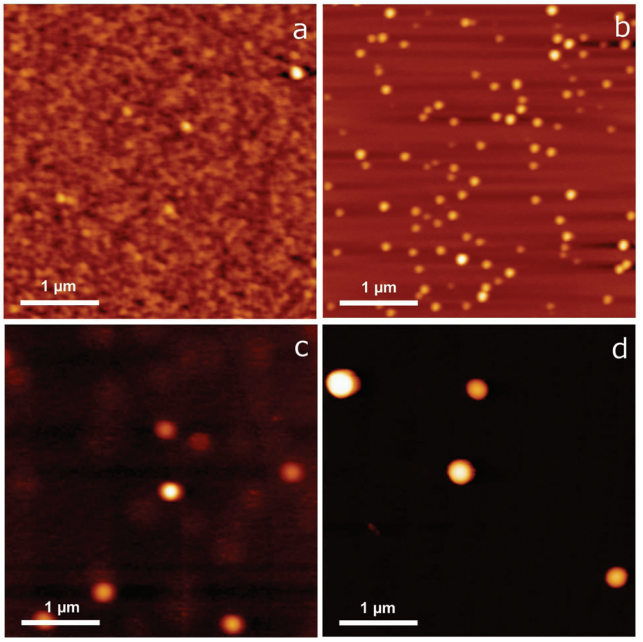

Figure 3. AFM images of Ay38/G4 assemblies with l = 4.02: (a) before irradiation; (b) irradiation at λ_{irr}= 313 nm; (c) irradiation at λ_{irr}= 335 nm; (d) irradiation at λ_{irr}= 380 nm.

yields assemblies which are not stable in solution even without irradiation. This is understandable as the absolute concentration of the free trans-dye stabilizing the assemblies in solution is already very low for such samples: a polymer concentrations as low as $c = 0.001$ g L^{-1} corresponds to excess dye concentrations in the range of 10^{-6} mol L^{-1}. Further, a higher polymer concentration of about 3-fold the standard concentration (c = 0.03 g L^{-1}) again yielded very similar results as presented, showing that the photoresponsiveness discussed herein is realizable over a relatively wide concentration range.

AFM is performed to provide complementary information on the size and structure of the Ay38/dendrimer assemblies. For this purpose, AFM images are recorded as shown in Figure 3, and the height and the average width of the particles are determined. This yields a volume of the assembly, which is converted into a hypothetical radius of a volume-equivalent spherical particle and compared to the hydrodynamic radius from DLS. Average radii determined from AFM data lie between R_{AFM} = 17 nm for the nonirradiated assemblies and R_{AFM} = 27 nm for λ_{irr} = 313 nm to R_{AFM} = 105 nm for λ_{irr} = 380, which shows that relative size changes are very similar to the ones observed in DLS. Evidently, AFM yields smaller sizes because the surface-deposited structure is dried. The size decrease upon drying is similar to values reported before, indicating a structure swollen by solvent in the solution shrinking upon drying.[54]

Irradiation with wavelengths larger than the absorption maximum decreases the degree of isomerization but does not decrease the particle size as depicted in Figure 2. For Ay38, the small radius decrease for irradiation with λ_{irr} = 405 nm is in the margin of error as the very strong scattering of the turbid particle dispersion does not allow measurements with high accuracy. Size changes due to irradiation are irreversible and thermal cis−trans isomerization does not lead to shrinkage of the particles back to the original size. Full reversibility can however be achieved by using pH as orthogonal trigger, ceasing electrostatic interaction of dye sulfonate and dendrimer amino groups.[52,59] This observation clarifies that the size change is not reversible by reisomerization of the dye molecules which may be understood in the same manner as coagulated latex particles cannot be redispersed after removal of surfactant.[60,69]

Figure 2b gives the ζ-potential as a function of irradiation wavelength for both dyes. The absolute value of the ζ-potential decreases with increasing fraction of cis-dye for Ay38 and Dy12. In this context it is important to note that the amount of salt is kept constant in all samples as all size changes are triggered by light irradiation being a noninvasive stimulus. The salt concentration is around c_{salt} = 0.75 mmol/L originating from pH adjustment, initial small counterions, and free dye.[70] A change in free dye concentration through dye dissociation is negligible as compared to the overall free dye concentration (<1%). Further, increasing the salt content by a factor of about 2 does not alter the light response of the system (which is realized for example when pH is used as a second trigger to dissolve and reassemble the assemblies whereafter the trend in assembly sizes and ζ-potential before and after irradiation are in agreement with the results presented here). This is in agreement with earlier results.[52,60]

The change in ζ-potential can hence be understood as follows: The amount of trans-dye available in solution decreases with irradiation at wavelengths up to the trans-isomer absorption maximum. As the dye molecules on the particles are in equilibrium with the solution, a lower total amount of trans-Ay38 in the sample leads to a lower concentration of particle-bound excess trans-dye (and trans-dye molecules free in solution). Because the cis-isomer has a much lower affinity to the particles, particle surface charge density and ζ-potential are reduced. Hence, particles with unchanged size would not be electrostatically stabilized anymore, and a partial coagulation process leads to higher particle sizes. This relationship is well evident in the data presented in Table 2 and Figure 2.[71]

It should also be noted that it is possible to increase the absolute value of the ζ-potential by irradidation at a wavelength corresponding to a lower fraction of cis-dye in the photoequilibrium (420 nm, ζ = −12 to ζ = −15 mV) as can be seen for Ay38 in Figure 2b. This is reasonable as the fraction of trans-dye in solution and thereby its absolute concentration is increased, which leads to a higher concentration of excess dye in the particles and thus an increased amount of charges per particle, i.e., a higher absolute value of the ζ-potential and a higher stability against coagulation. This is important to stabilize the particles as ζ-potential values of around ζ = −10 mV are not sufficient to guarantee long-term stability. The same effect can also be achieved by adding more trans-dye stock solution. Such behavior is a very interesting feature, as it allows to first adjust the particles to a desired size and thereafter increase the stability of the particles. Very promising may be the perspective to use dyes with reactive handles to fix the dyes on the particle. Thereafter, no free dye molecules might be required in solution if they disturb possible applications.

Nanoparticles exhibit a high surface area, which has to be stabilized, in this case electrostatically. The particle surface relative to its initial value can be calculated under the assumption that the overall particle volume and density are constant, which is expected to hold in this case as no precipitation occurs; i.e., all material stays in solution, but only the particle size increases. The relative surface area of the particles can be calculated from the hydrodynamic radii from the light scattering data by the relation given in eq IV:

$$V_1 = N_1 \frac{4}{3}\pi {R_{h1}}^3 = N_2 \frac{4}{3}\pi {R_{h2}}^3 = V_2 \text{ and}$$

$$\frac{S_1}{S_2} = \frac{N_1 4\pi {R_{h1}}^2}{N_2 4\pi {R_{h2}}^2} = \frac{R_{h2}}{R_{h1}} \qquad \text{(IV)}$$

where V_1 and S_1 are the total volume and surface of all particles in the sample and R_{h1} and N_1 the hydrodynamic radius and the number of particles before irradiation with a certain wavelength. The index 2 stands for the same parameters after irradiation with light at a certain wavelength.

Therefore, it is very interesting to investigate whether there is a correlation between the absolute concentration of trans-dye in solution and the relative total particle surface. Figure 4 shows the connection between surface area and absolute concentration of trans-dye in the samples (compare Table 2). Especially Ay38 (Figure 4a) shows that the absolute concentration of trans-dye decreases in the same way as the total particle surface; i.e., the relative changes for both curves are similar. This is an indication that the process is surface-controlled. The behavior of this system may be compared to surfactant-stabilized latex particles when the surfactant is removed. For Dy12 (Figure 4b), the overall behavior is also comparable. The decrease in surface area only starts after the dye concentration is lowered below a certain threshold value, which also corresponds to the higher initial value of the ζ-potential. Still, after the changes in hydrodynamic radius at λ_{irr} = 375 and λ_{irr} = 395 nm, the curves for the absolute dye

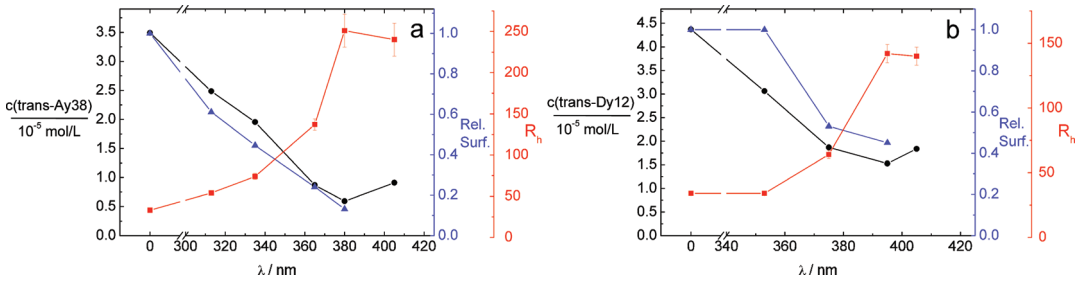

Figure 4. Absolute concentration of trans-dye (black circles) and reduction of total particle surface (blue triangles) and hydrodynamic radii (red squares). (a) Ay38 and (b) Dy12 samples from Figure 2 after irradiation at varying wavelength. The error for relative surfaces is about ±5% and for absolute concentrations of free dye ±10%.

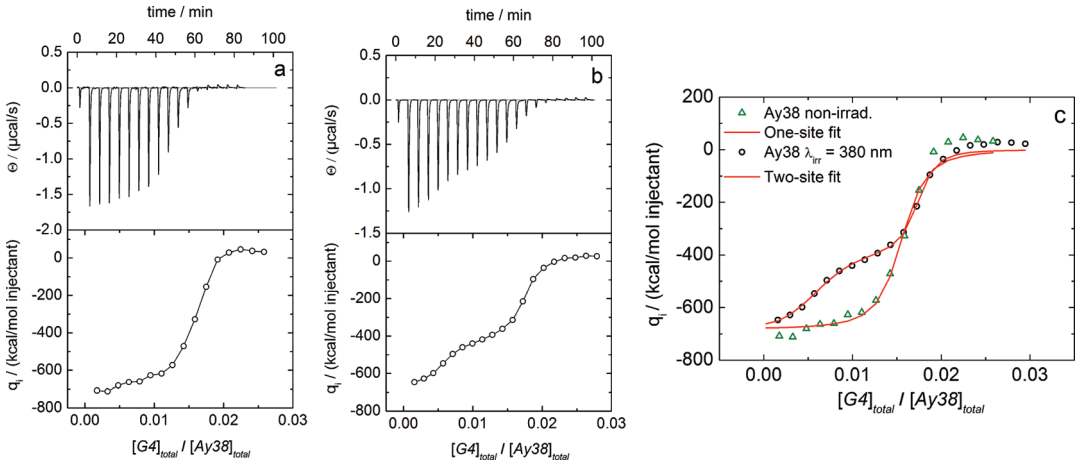

Figure 5. Isothermal titration calorimetry to study the assembly formation of cis- and trans-Ay38 (titrant, cell) with G4 PAMAM dendrimer (titrator, syringe); reaction heats (top) and the reaction enthalpies per mol of injectant (bottom, raw heat divided by the molar amount of injectant per injection): (a) trans-Ay38 ($[Ay38]_{cell}$ = 30.65 μmol/L) into G4 dendrimer ($[G4]_{syringe}$ = 5.46 μmol/L); (b) 83% cis-Ay38 ($[Ay38]_{cell}$ = 34.05 μmol/L) into G4 dendrimer ($[G4]_{syringe}$ = 5.46 μmol/L); (c) fit of the raw data of the two experiments. One-site model is used for trans-Ay38 (nonirradiated) and two-site for 83% cis-Ay38 (λ_{irr} = 380 nm).

concentration (Figure 4b, black line) and relative surface (Figure 4b, blue line) exhibit similar changes, showing that the same concept holds for both dye building blocks.

In conclusion of this section, we could prove that the surface area stabilized by excess dye molecules is key to the growth process, i.e., determines the size of the particles. A reduced surface charge density leads to a decrease of surface and thereby a size increase, as was shown by AFM, DLS, and ζ-potential measurements.

C. Binding Equilibria, Enthalpies, and Entropies of Assembly Formation. To understand why the ability of the trans-dye to bind overstoichiometrically to electrostatically self-assembled particles is higher than of the cis-dye, measurements of thermodynamic parameters via ITC is an excellent pathway. Figure 5, Figure 6, and Table 3 show ITC raw data and analysis of titrations of G4 PAMAM dendrimer in irradiated and nonirradiated Ay38 and Dy12 solutions.

First, nonirradiated samples will be discussed. From Figures 5a and 6a it is evident that the association of Ay38 and Dy12 can be described by a one-site-model, which is described elsewhere.[54,72] A one-site model considers the equilibrium described in eq V with Ay38 as example:

$$N(\mathrm{Ay38})_{\mathrm{trans}} + \mathrm{dendrimer} \rightarrow (\mathrm{Ay38_{trans}})_N\mathrm{-dendrimer} \quad (\mathrm{V})$$

It should be noted that for ITC measurements with azo dyes and dendrimers the enthalpies and stoichiometries are usually very accurate, whereas the equilibrium constants and therefore the entropies are less accurate. That is due to the high binding affinities in combination with the concentration limitation for measurements that do not allow measurements at very low dye concentrations because of adsorption of the dye molecules to the cell walls.[54] Therefore, a moderate dye concentration ($c_{dye} \approx$ 3 μmol/L) was chosen to obtain best accuracy in view of the mentioned limitations.

Table 3 shows that the binding of both dyes to the dendrimer is exothermic with a binding enthalpy per dye around ΔH_{perdye} = −43 kJ/mol, which indicates that electrostatic binding and $\pi-\pi$ interactions contribute to the binding process.[54] The binding constant for Dy12 is around 1 order of magnitude higher than for Ay38 (K_1^{Dy12} = 4 × 10^7 L/mol compared to K_1^{Ay38} = 4 × 10^6 L/mol). One reason for the stronger binding is the lower loss of entropy for Dy12, which is evident in Table 3.

Both dyes can bind slightly overstoichiometrically to the dendrimer as becomes evident from the stoichiometry parameter of 66 dyes per dendrimer molecule found for both systems (63 is the theoretical value for electrostatic binding). To investigate the role of the thermodynamic parameters in relation to the assembly formation, different dyes are compared, and in addition to the two previously mentioned dyes, ITC was also conducted with the dye counterion ABDS (compare Scheme 1). This is not discussed in the preceding sections as it does not form stable assemblies with

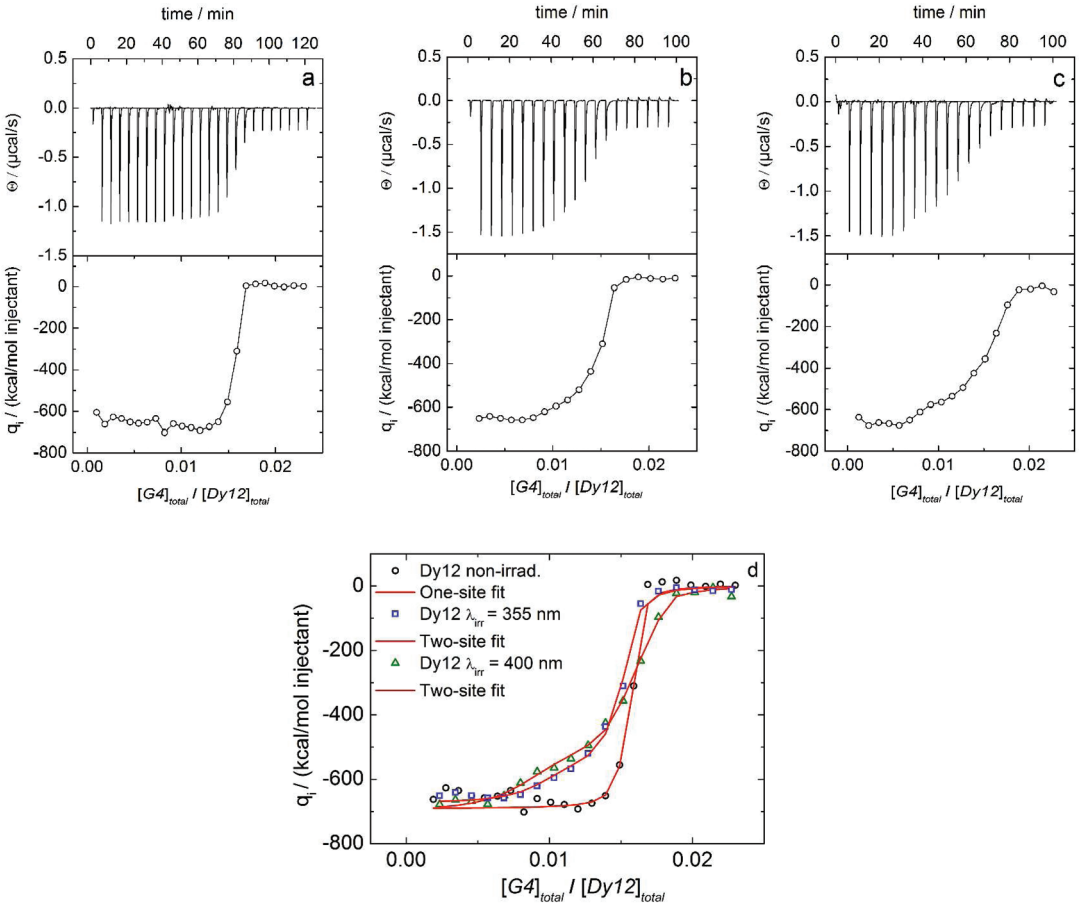

Figure 6. Isothermal titration calorimetry to study the assembly formation of cis- and trans-Dy12 (titrand, cell) with G4 PAMAM dendrimer (titrand, syringe); reaction heats (top) and the reaction enthalpies per mol of injectant (bottom, raw heat divided by the molar amount of injectant per injection): (a) trans-Dy12 ($[Dy12]_{cell}$ = 33.05 μmol/L) into G4 dendrimer ($[G4]_{syringe}$ = 3.40 μmol/L); (b) 30%cis- Dy12 ($[Dy12]_{cell}$ = 33.05 μmol/L) into G4 dendrimer ($[G4]_{syringe}$ = 3.40 μmol/L); (c) 65%cis-Dy12 ($[Dy12]_{cell}$ = 33.05 μmol/L) into G4 dendrimer ($[G4]_{syringe}$ = 3.40 μmol/L); (d) fit of the raw data. One-site model is used for trans-Dy12 (a) and two-site model for trans/cis-Dy12 mixtures (b, c).

Table 3. ITC Data for ABDS, Ay38, and Dy12[a]

titrand	λ_{irr}/nm	ΔH_1/(kJ/mol)	K_1/(L/mol)	N_1	$T\Delta S_1$/(kJ/mol)	ΔH_2/(kJ/mol)	K_2/(L/mol)	N_2	$T\Delta S_2$/(kJ/mol)
ABDS[c]	–	−18.2	5×10^4	52	8.65				
ABDS[c]	325[b]	−18.5	2×10^4	56	6.14				
Ay38	–	−42.5	4×10^6	66	−4.97				
Ay38	380	−45.3	2×10^7	20	−3.16	−26.2	4×10^6	39	11.63
Dy12	–	−43.9	4×10^7	66	−0.56				
Dy12	355	−40.8	1×10^8	43	5.03	−32.9	2×10^6	26	3.52
Dy12	395	−44.4	4×10^7	36	−1.06	−32.2	2×10^6	30	3.53

[a] Errors: One-site model: (a) ΔH: 2−3%; (b) K: 20−40%; (c) N: 3−5%; (d) $T\Delta S$: 20−30%. Two-site model: (a) ΔH: 3−5%; (b) K: 20−60%; (c) N: 10% ; (d) $T\Delta S$: 20−60%. [b] The fraction of cis-isomer is around 45% in this case. [c] Errors for ABDS are only 5% for K.

the dendrimer. The reason is most likely that the binding energy is too low (ΔH = −18 kJ/mol) without sufficient entropic compensation. This suggests that a certain minimum of energy is required to form stable assemblies.

Comparing the data of the nonirradiated and the irradiated samples gives valuable insight into the differences between trans- and cis-dye. Already from the raw data it is evident that trans- and cis-isomers of Ay38 and Dy12 exhibit different binding patterns, as there is a step in the binding isotherm for the irradiated samples. It can be fitted well with a two-site model. The two-site model can be described by eq VI:[73]

$$N\mathrm{Ay38_{trans}} + M\mathrm{Ay38_{cis}} + \mathrm{dendrimer} \rightarrow (\mathrm{Ay38_{trans}})_N(\mathrm{Ay38_{cis}})_M\mathrm{-dendrimer} \quad \text{(VI)}$$

For the data analysis, thermal cis−trans reisomerization is an issue here, as during the measurement, cis-dye can already reisomerize to the trans-state thermally and lead to higher slopes.

dx.doi.org/10.1021/ma200538e |Macromolecules 2011, 44, 4452–4461

Higher slopes lead to higher binding constants and thus overestimate all binding constants in the two-site process somewhat. Therefore, the absolute values of the two-site binding constants and entropies should only be compared between trans- and cis-isomer and not on an absolute scale to the more accurate values derived from the one-site model for pure trans-dye.

The reaction enthalpy for the first binding process is almost identical to the values reported above for the samples where the dendrimer is injected into nonirradiated trans-Ay38 and trans-Dy12 solutions. Therefore, this first process most likely corresponds to trans-dye ($\Delta H_1 \approx -43$ kJ/mol, $K_1 \approx 10^7$ L/mol), whereas the second process with the lower binding affinity originates from binding of cis-dye to the dendrimer ($\Delta H_2 \approx -26$ to -33 kJ/mol, $K_2 \approx 10^6$ L/mol). Thus, it is worthwhile to discuss the contributions to the binding strength for both isomers, which originate mainly from electrostatic interaction and $\pi-\pi$ stacking, while hydrophobic interactions, differences in hydration due to molecule polarity, and geometric effects may also play a role. As the number of charges does not change, the cause for the change in reaction enthalpy and binding strength likely lies in reduced mutual $\pi-\pi$ or hydrophobic interactions of the dye counterions. This may be caused by the fact that the cis-isomer, in addition to the different geometry of the dye isomers, is more polar and hydrophilic than the trans-isomer[44,47] and thus is most likely hydrated to a higher extent than the more hydrophobic trans-isomer. A higher degree of hydration of the cis-isomer leads to a higher affinity to the water phase as compared to the development of mutual interactions based on $\pi-\pi$ stacking or hydrophobicity, the latter being more expressed for trans-dye molecules. The mutual interaction among the dye molecules favoring overbinding is thus more expressed for the trans-isomers, as becomes evident by the higher interaction energy and binding strength. Hence, this is the source for the lower ability for overstoichiometric binding of the cis-isomer as compared to the trans-form. Therefore, the trans-dye overbinds to a larger extent. This is in good agreement with the finding above that particles grow when the fraction of cis-isomers in the sample increases. If trans-dye is converted to cis-dye, less overbinding takes place leading to dye dissociation from the particle and hence particle combination and thus growth as discussed above. The difference in enthalpy is larger for Ay38 than for Dy12. This explains why the size changes for Dy12 are less than for Ay38.

CONCLUSION

In conclusion, we have shown that electrostatically self-assembled nanoparticles from ionic azo-dyes and macroions can be size-controlled by irradiation with UV-light. UV-light irradiation causes charge reduction and size increase of the particles. The size increase is induced by trans−cis isomerization of the dye leading to a weaker mutual interaction of the dye molecules. This causes a loss of electrostatic stabilization of the nanoparticles, which is compensated by reducing the total amount of surface that needs to be stabilized through growth of the nanoparticles. With this study, we established a new route to prepare size-controllable nanoparticles with UV light as a trigger, whereby the desired size can be precisely controlled through the choice of the irradiation wavelength. Hence, this is potentially a powerful and versatile concept for future applications.

AUTHOR INFORMATION

Corresponding Author

*Fax: 49-9131-85 28307. E-mail: Franziska.Groehn@chemie.uni-erlangen.de.

ACKNOWLEDGMENT

Financial support of Deutsche Forschungsgemeinschaft (DFG), Verband der Chemischen Industrie (VCI), and the Interdisciplinary Center for Molecular Materials (ICMM, University Erlangen-Nürnberg) is gratefully acknowledged. We are thankful to Prof. Helmut Ritter, University Düsseldorf, for letting us perform ITC measurements in his laboratory.

REFERENCES

(1) Ringsdorf, H.; Schlarb, B.; Venzmer, J. *Angew. Chem., Int. Ed.* **1988**, *27*, 113–158.
(2) Sijbesma, R. P.; Beijer, F. H.; Brunsveld, L.; Folmer, B. J. B.; Hirschberg, J. H. K. K.; Lange, R. F. M.; Lowe, J. K. L.; Meijer, E. W. *Science* **1997**, *278*, 1601–1604.
(3) Antonietti, M.; Förster, S. *Adv. Mater.* **2003**, *15*, 1323–1333.
(4) Percec, V.; Dulcey, A. E.; Balagurusamy, V. S. K.; Miura, Y.; Smidrkal, J. *Nature* **2004**, *430*, 764–768.
(5) Kaiser, T. E.; Wang, H.; Stepanenko, V.; Würthner, F. *Angew. Chem., Int. Ed.* **2007**, *46*, 5541–5544.
(6) Wu, C.; Gao, J. *Macromolecules* **2000**, *33*, 645–646.
(7) Elmahdy, M. M.; Dou, X.; Mondeshki, M.; Floudas, G.; Butt, H. J.; Spiess, H. W.; Müllen, K. *J. Am. Chem. Soc.* **2008**, *130*, 5311–5319.
(8) Lee, E.; Kim, J. K.; Lee, M. *Angew. Chem., Int. Ed.* **2008**, *47*, 6375–6378.
(9) Becherer, M. S.; Schade, B.; Böttcher, C.; Hirsch, A. *Chem.—Eur. J.* **2009**, *15*, 1637–1648.
(10) Xu, Y.; Bolisetty, S.; Ballauff, M.; Müller, A. H. E. *J. Am. Chem. Soc.* **2009**, *131*, 1640–1641.
(11) Grzybowski, B. A.; Wilmer, C. E.; Kim, J.; Bowne, K. P.; Bishop, K. J. M. *Soft Matter* **2009**, *5*, 1110–1128.
(12) Lemmers, M.; Sprakel, J.; Voets, I. K.; van der Gucht, J.; Cohen Stuart, M. A. *Angew. Chem., Int. Ed.* **2010**, *49*, 708–711.
(13) Berret, J.-F. *Macromolecules* **2007**, *40*, 4260–4266.
(14) Balazs, A. C.; Emrick, T.; Russell, T. P. *Science* **2006**, *314*, 1107–1110.
(15) Gröhn, F.; Gu, X.; Grüll, H.; Meredith, J. C.; Nisato, G.; Bauer, B. J.; Karim, A.; Amis, E. J. *Macromolecules* **2002**, *35*, 4852–4854.
(16) Yan, M.; Fresnais, J.; Berret, J.-F. *Soft Matter* **2010**, *6*, 1997–2005.
(17) Discher, D. E.; Eisenberg, A. *Science* **2002**, *297*, 967–973.
(18) Thünemann, A. F.; General, S. *Macromolecules* **2001**, *34*, 6978–6984.
(19) Ling, X. Y.; Reinhoudt, D. N.; Huskens, J. *Pure Appl. Chem.* **2009**, *81*, 2225–2233.
(20) Konstantatos, G.; Howard, I.; Fischer, A.; Hoogland, S.; Clifford, J.; Klem, E.; Levina, L.; Sargent, E. H. *Nature* **2006**, *442*, 180–183.
(21) Feng, X.; Pisula, W.; Kudernac, T.; Wu, D.; Zhi, L.; De Feyter, S.; Müllen, K. *J. Am. Chem. Soc.* **2009**, *131*, 4439–4448.
(22) Neumann, B.; Huber, K.; Pollmann, P. *Phys. Chem. Chem. Phys.* **2000**, *2*, 3687–3695.
(23) Moreno-Villoslada, I.; Torres-Gallegos, C.; Araya-Hermosilla, R.; Nishide, H. *J. Phys. Chem. B* **2010**, *114*, 4151–4158.
(24) Moreno-Villoslada, I.; Jofre, M.; Miranda, V.; Gonzalez, R.; Sotelo, T.; Hess, S.; Rivas, B. L. *J. Phys. Chem. B* **2006**, *110*, 11809–11812.
(25) Percec, V.; Glodde, M.; Peterca, M.; Rapp, A.; Schnell, I.; Spiess, H. W.; Bera, T. K.; Miura, Y.; Balagurusamy, V. S. K.; Aqad, E.; Heiney, P. A. *J. Am. Chem. Soc.* **2007**, *129*, 11265–11278.
(26) Pochan, D. J.; Chen, Z.; Cui, H.; Hales, K.; Qi, K.; Wooley, K. L. *Science* **2004**, *306*, 94–97.
(27) Liu, X.; Kim, J.-S.; Wu, J.; Eisenberg, A. *Macromolecules* **2005**, *38*, 6749–6751.
(28) Nikolic, M. S.; Olsson, C.; Salcher, A.; Kornowski, A.; Rank, A.; Schubert, R.; Frömsdorf, A.; Weller, H.; Förster, S. *Angew. Chem., Int. Ed.* **2009**, *48*, 2752–2754.

(29) Yuan, X.; Jiang, M.; Zhao, H.; Wang, M.; Zhao, Y.; Wu, C. *Langmuir* **2001**, *17*, 6122–6126.
(30) Duschner, S.; Störkle, D.; Schmidt, M.; Maskos, M. *Macromolecules* **2008**, *41*, 9067–9071.
(31) Stoerkle, D.; Duschner, S.; Heimann, N.; Maskos, M.; Schmidt, M. *Macromolecules* **2007**, *40*, 7998–8006.
(32) Ou, Z.; Muthukumar, M. *J. Chem. Phys.* **2006**, *124*, 154902.
(33) Thünemann, A. F.; Müller, M.; Dautzenberg, H.; Joanny, J.-F.; Loewen, H. *Adv. Polym. Sci.* **2004**, *166*, 113–171.
(34) Beck, J. B.; Rowan, S. J. *J. Am. Chem. Soc.* **2003**, *125*, 13922–13923.
(35) Rakotondradany, F.; Whitehead, M. A.; Lebuis, A. M.; Sleiman, H. F. *Chem.—Eur. J.* **2003**, *9*, 4771–4780.
(36) Yagai, S.; Kitamura, A. *Chem. Soc. Rev.* **2008**, *37*, 1520–1529.
(37) Zhao, Y.-L.; Stoddart, J. F. *Langmuir* **2009**, *25*, 8442–8446.
(38) Tazawa, T.; Yagai, S.; Kikkawa, Y.; Karatsu, T.; Kitamura, A.; Ajayaghosh, A. *Chem. Commun.* **2010**, *46*, 1076–1078.
(39) Yuan, X.; Fischer, K.; Schärtl, W. *Langmuir* **2005**, *21*, 9374–9380.
(40) Yuan, X.; Schnell, M.; Muth, S.; Schaertl, W. *Langmuir* **2008**, *24*, 5299–5305.
(41) Lee, C. T., Jr.; Smith, K. A.; Hatton, T. A. *Macromolecules* **2004**, *37*, 5397–5405.
(42) Hubbard, F. P.; Abbott, N. L. *Langmuir* **2007**, *23*, 4819–4829.
(43) Sakai, H.; Matsumura, A.; Yokoyama, S.; Saji, T.; Abe, M. *J. Phys. Chem. B* **1999**, *103*, 10737–10740.
(44) Lin, Y.; Cheng, X.; Qiao, Y.; Yu, C.; Li, Z.; Yana, Y.; Huang, J. *Soft Matter* **2010**, *6*, 902–908.
(45) Eastoe, J.; Vesperinas, A. *Soft Matter* **2005**, *1*, 338–347.
(46) Eastoe, J.; Vesperinas, A.; Donnewirth, A.-C.; Wyatt, P.; Grillo, I.; Heenan, R. K.; Davis, S. *Langmuir* **2006**, *22*, 5299–5305.
(47) Ikeda, T.; Mamiya, J.; Yu, Y. *Angew. Chem., Int. Ed.* **2007**, *46*, 506–528.
(48) Yu, B.; Jiang, X.; Wang, R.; Yin, J. *Macromolecules* **2010**, *43*, 10457–10465.
(49) Nalluri, S. K. M.; Ravoo, B. J. *Angew. Chem., Int. Ed.* **2010**, *49*, 5371–5374.
(50) Tomatsu, I.; Hashidzume, A.; Harada, A. *J. Am. Chem. Soc.* **2006**, *128*, 2226–2227.
(51) Gröhn, F.; Klein, K.; Brand, S. *Chem.—Eur. J.* **2008**, *14*, 6866–6869.
(52) Willerich, I.; Gröhn, F. *Chem.—Eur. J.* **2008**, *14*, 9112–9116.
(53) Gröhn, F. *Macromol. Chem. Phys.* **2008**, *209*, 2295–2301.
(54) Willerich, I.; Ritter, H.; Gröhn, F. *J. Phys. Chem. B* **2009**, *113*, 3339–3354.
(55) Li, Y.; Yildiz, U. H.; Müllen, K.; Gröhn, F. *Biomacromolecules* **2009**, *10*, 530–540.
(56) Yildiz, U. H.; Koynov, K.; Gröhn, F. *Macromol. Chem. Phys.* **2009**, *210*, 1678–1690.
(57) Gröhn, F.; Klein, K.; Koynov, K. *Macromol. Rapid Commun.* **2010**, *31*, 75.
(58) Gröhn, F. *Soft Matter* **2010**, *6*, 4296–4302.
(59) Willerich, I.; Li, Y.; Gröhn, F. *J. Phys. Chem. B* **2010**, *114*, 15466–15476.
(60) Willerich, I.; Gröhn, F. *Angew. Chem., Int. Ed.* **2010**, *49*, 8104–8108.
(61) Ruthard, C.; Maskos, M.; Kolb, U.; Gröhn, F. *Macromolecules* **2009**, *42*, 830–840.
(62) Reinhold, F.; Kolb, U.; Gröhn, F. *Langmuir* **2009**, *25*, 1345–1351.
(63) Tomalia, D. A.; Baker, E.; Dewald, J.; Hall, M.; Kallos, G.; Martin, S.; Raeck, J.; Ryder, J.; Smith, P. *Macromolecules* **1986**, *19*, 2466–2468.
(64) Robinson, C.; Mills, H. A. T. *Proc. R. Soc. London, A* **1931**, *131*, 576–595.
(65) Clarke, H. T. *J. Org. Chem.* **1971**, *36*, 3816–3819.
(66) Provencher, S. W. *Comput. Phys. Commun.* **1982**, *27*, 229–242.
(67) Fischer, E. *J. Phys. Chem.* **1967**, *71*, 3704–3707.
(68) Petrak, K.; Douglas, P.; Leyshon, L. L. *J. Appl. Polym. Sci.* **1986**, *31*, 553–565.
(69) Zelenev, A.; Matijevid, E. *Colloids Surf., A* **1997**, *125*, 171–179.
(70) For example, c(NaCl from pH preparation) = 6.32×10^{-4} mol/L, c(NaCl from initial counterions) = 8.5×10^{-5} mol/L; c(free dye) = 3.5×10^{-5} (c(charges, free dye) = 7×10^{-5}).
(71) Note that the ζ-potential depends on charge/radius; hence also a constant total charge would lead to a decreased absolute value of the ζ-potential when the particle size increases. It is however safe to refer to a charge density or an effective charge density, which would still be lower for the larger particle, even for constant charge. This refers to the ζ-potential measured at the shear plane.
(72) Wiseman, T.; Williston, S.; Brandts, J. F.; Lin, L. N. *Anal. Biochem.* **1989**, *179*, 131–137.
(73) ITC Data Analysis in Origin, MicroCal, Version 7.0, Jan 2004.